Purely Spintronic Leaky Integrate-and-Fire Neurons

Wesley H. Brigner[1], Naimul Hassan[1], Xuan Hu[1], Christopher H. Bennett[2], Felipe Garcia-Sanchez[3], Matthew J. Marinella[5], Jean Anne C. Incorvia[5], Joseph S. Friedman[1]
[1]Electrical and Computer Engineering, University of Texas at Dallas, Richardson, TX, United States
[2]Sandia National Laboratories, Albuquerque, NM, United States
[3]Department of Applied Physics, University of Salamanca, Salamanca, Spain
[4]Electrical and Computer Engineering, University of Texas at Austin, Austin, TX, United States
[5]Electrical and Computer Engineering, Arizona State University, Tempe, AZ, United States

Abstract—**Neuromorphic computing promises revolutionary improvements over conventional systems for applications that process unstructured information. To fully realize this potential, neuromorphic systems should exploit the biomimetic behavior of emerging nanodevices. In particular, exceptional opportunities are provided by the non-volatility and analog capabilities of spintronic devices. While spintronic devices that emulate neurons have been previously proposed, they require complementary metal-oxide semiconductor (CMOS) technology to function. In turn, this significantly increases the power consumption, fabrication complexity, and device area of a single neuron. This work reviews three previously proposed CMOS-free spintronic neurons designed to resolve this issue.**

Index Terms—**Artificial neural network, Neuromorphic computing, Leaky integrate-and-fire neuron**

I. Introduction

In the human brain, a neuron integrates a series of electrical spikes through its axons and, when enough of these current pulses have been integrated, it releases a spike of its own from the soma (cell body) and through its dendrites to the axons of other neurons. Synapses, on the other hand, provide electrical connectivity between the axons of one neuron and the dendrites of other neurons.

To mimic the brain, neuromorphic systems typically contain artificial neuron and synapse analogs. Such systems can be emulated using software on von Neumann computers [1],[2]; however, due to the fact that complementary metal oxide semiconductor (CMOS) technology, which is the primary technology used in standard von Neumann computers, was not specifically designed to implement the required behavior, these systems consume considerably more energy than an actual human brain [3]. Novel CMOS-based systems can also be used to implement neuromorphic systems [4],[5], but again, CMOS was not specifically designed to match the needs for neuromorphic computing and such chips are highly inefficient.

To resolve the issues of inefficiency and high power consumption, neuromorphic-inspired beyond-CMOS devices have garnered a considerable amount of attention in the scientific community. Since synapses only require non-volatility and a variable resistance, several beyond-CMOS synapses have already been proposed [6]-[9]. On the other hand, fewer beyond-CMOS neurons have been proposed due to the unique challenges in emulating the leaky integrate-and-fire (LIF) neuron model [8]-[11]. While these previously proposed spintronic neurons efficiently provide leaking, integrating, firing, and lateral inhibition, electrical connectivity between the input and output ports results in a need for CMOS circuitry between perceptron layers.

This paper reviews three recently proposed neurons designed to eliminate the need for CMOS circuitry, thereby enabling a monolithic, purely spintronic neuromorphic architecture. A brief background to the field of neuromorphic computing is provided in section 2, while background on spintronic synapses and a review of the aforementioned neurons is presented in section 3. A discussion of a purely spintronic neural network is provided in section 4, and finally, conclusions are provided in section 5.

II. Background

Due to the fact that novel technologies and architectures are still required to be compatible with currently existing fabrication

Wesley H. Brigner (email: Wesley.Brigner@utdallas.edu), Naimul Hassan (email: Naimul.Hassan@utdallas.edu), Xuan Hu (email: Xuan.Hu@utdallas.edu), and Joseph S. Friedman (email: Joseph.Friedman@utdallas.edu) are with the University of Texas at Dallas, Richardson, TX 75080 USA.

Christopher H. Bennett (email: cbennet@sandia.gov) is with Sandia National Laboratories, Albuquerque, NM 87185 USA.

Felipe Garcia-Sanchez (email: f.garcia@inrim.it) was with the Istituto Nazionale Di Ricerca Metrologica, and is now with the Universidad de Salamanca, 37008 Salamanca, Spain.

Matthew J. Marinella (email: m@asu.edu) is with Arizona State University, Tempe, AZ 85287 USA.

Jean Anne C. Incorvia (email: incorvia@austin.utexas.edu) is with the University of Texas at Austin, Austin, TX 78705 USA.

978-1-6654-8485-5/22/$31.00 ©2022 IEEE

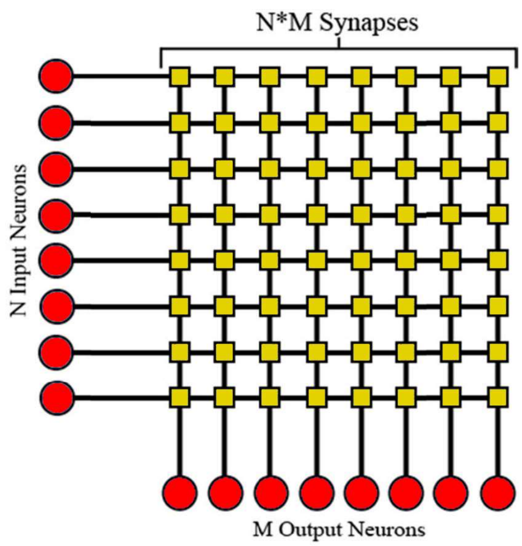

Fig. 1. NxM crossbar array consisting of N+M neurons and N*M synapses.

techniques, many beyond-CMOS technologies, including the previously proposed neuromorphic structures discussed in this work, are designed using a crossbar array structure.

A. Crossbar Array

An NxM crossbar array consists of N horizontal wires (word lines) and M vertical wires (bit lines). For a layer in a neuromorphic system, a single input neuron will be attached to each word line and a single output neuron will be attached to each bit line, resulting in N+M total neurons. Likewise, a single synapse exists at each word and bit line intersection to provide connectivity between the input and output neurons for a total of N*M synapses. The resistance states of these synapses, which are capable of being finely tuned during training, determine the weighting between the input and output neurons, and, ultimately, the overall functionality of the neuromorphic layer [7]. This structure is illustrated in Figure 1.

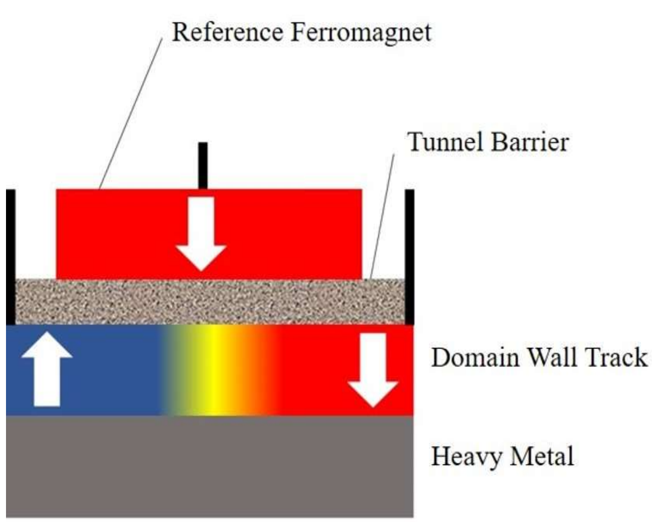

Fig. 2. DW-MTJ synapse with wide tunnel barrier for analog resistance states.

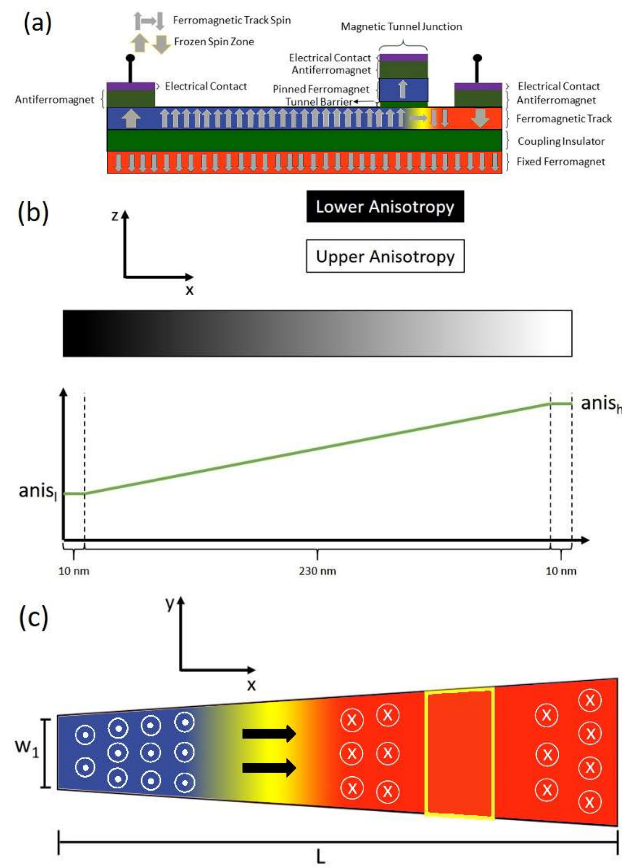

Fig. 3. (a) Side view of the neuron with dipolar coupling field. (b) Side view of the neuron with graded anisotropy illustrating the anisotropy gradient instead of magnetization. (c) Structure of the neuron with shape-based DW drift.

B. Leaky Integrate-and-Fire Neuron

A biologically-accurate neuron model is the leaky integrate-and-fire (LIF) neuron model, which is a considerable improvement over the previous integrate-and-fire (IF) neurons [1]. LIF neurons should implement three primary functionalities. As implied by the name, these functionalities are integrating, leaking, and firing. When an energy spike is fed into the input of an LIF neuron, the neuron should store the energy from the spike. However, when no energy is applied to the input of the neuron, it should gradually dissipate the stored energy. Finally, once the stored energy has reached a certain threshold, the neuron should suddenly release an output energy spike and reset its state to the initial state.

III. Domain Wall Magnetic Tunnel Junction

A domain wall magnetic tunnel junction (DW-MTJ) consists of a “free” ferromagnetic layer containing two magnetic domains separated by a domain wall (DW) such that the position of the DW determines the MTJ resistance. When the DW, which can be moved using a current, passes underneath, the MTJ switches between the parallel (conductive) and anti-parallel (resistive) states.

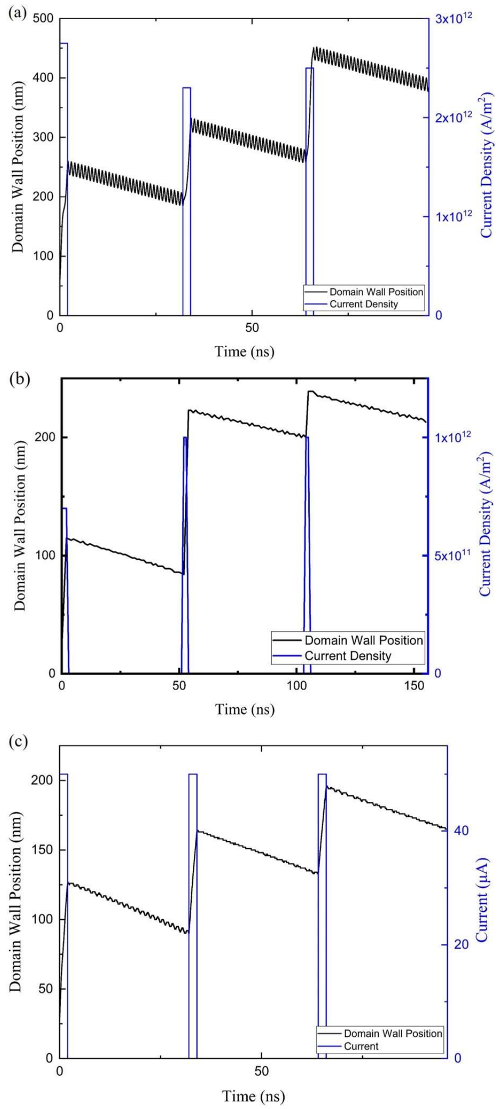

Fig. 4. (a) Combined integrating and leaking characteristics of a neuron implemented using a dipolar coupling field. (b) Combined integrating and leaking characteristics of a neuron with anisotropy gradient. (c) Combined integrating and leaking characteristics of a neuron with shape-based DW drift.

A. DW-MTJ Synapse and Neuron Integration

This synapse, which is shown in Figure 2, consists of a long tunnel barrier that covers a large portion of the DW track [8], [9], allowing the device to exhibit analog resistance states. When a current flows through the DW track, the DW shifts from one end of the track to the other. When used in a DW-MTJ neuron, this DW motion represents integration through an increase in stored energy.

B. Leaking with a DW-MTJ Neuron

Leaking can be achieved using one of three methods. With the first method, a ferromagnet is placed underneath the DW track and provides a dipolar coupling field, as illustrated in Figure 3a. When a dipolar coupling field is applied parallel to a magnetic domain's magnetization state, the field causes the domain to expand. Conversely, if the same field is applied antiparallel to a magnetic domain's magnetization state, the field will cause the domain to shrink. Therefore, a magnetic field applied to a DW track along the same axis as the two antiparallel magnetic domains will cause the DW to shift from one side of the track to the other. The dipolar coupling field provided by the aforementioned ferromagnet allows the DW to shift from one end of the track to the other in the absence of any current. As illustrated in the micromagnetic simulation results of Figure 4a, when a current is applied from right to left through the DW track, the DW shifts from left to right. However, when no current is applied, the DW gradually shifts from right to left [12].

In the second method, illustrated in Figure 3b, the DW track contains a magnetocrystalline anisotropy gradient, which can be implemented using a thickness and/or composition gradient [15]-[17]. When the DW is in a region of the track with a higher anisotropy value, it exists in a higher energy state, and when the DW is in a region of the track with a lower anisotropy value, it exists in a lower energy state. Therefore, the anisotropy gradient generates an energy landscape that is more favorable to the DW existing on one side of the track than the other. Figure 4b demonstrates micromagnetic simulation results of the combined leaking and integrating characteristics of a graded anisotropy neuron. As with the neuron with a dipolar coupling field, a current passed from right to left in the device causes a rapid shift in the DW position from left to right. When no current is applied, the DW slowly leaks from right to left [13].

With the third method, the sides of the DW track are angled to form a trapezoidal track instead of a rectangular track, as demonstrated in Figure 3c. Similar to the anisotropy gradient neuron, the DW exists in a higher energy state when it is in the wider region than when it is in the narrower region. Therefore, the DW will shift from the wide portion of the DW track to the narrow portion without any externally-applied stimuli. When applying a current from right to left through the device, as in Figure 4c, the DW shifts from left to right. When no current is passed through the device, the energy landscape present in the DW track forces the DW to shift from right to left [14].

Finally, the fabrication approaches for these three methods are evaluated in Table I. The neuron with the dipolar coupling field has the simplest fabrication process for each layer; however, it requires two additional layers – one being the

TABLE I. COMPARISON OF FABRICATION APPROACHES

Leaking Mechanism	**Dipolar Coupling Field**	**Anisotropy Gradient**	**Shape Gradient**
Fabrication Approach	Additional ferromagnet provides dipolar coupling field	Ga+ ion irradiation gradient of DW track	Lithography of non-rectangular shape
Advantages	Simple fabrication of each layer	No extra material layers	No extra material layers
Disadvantages	Requires additional material layers	Requires additional fabrication steps to irradiate DW track	Requires gradient of DW track width. Increased area overhead

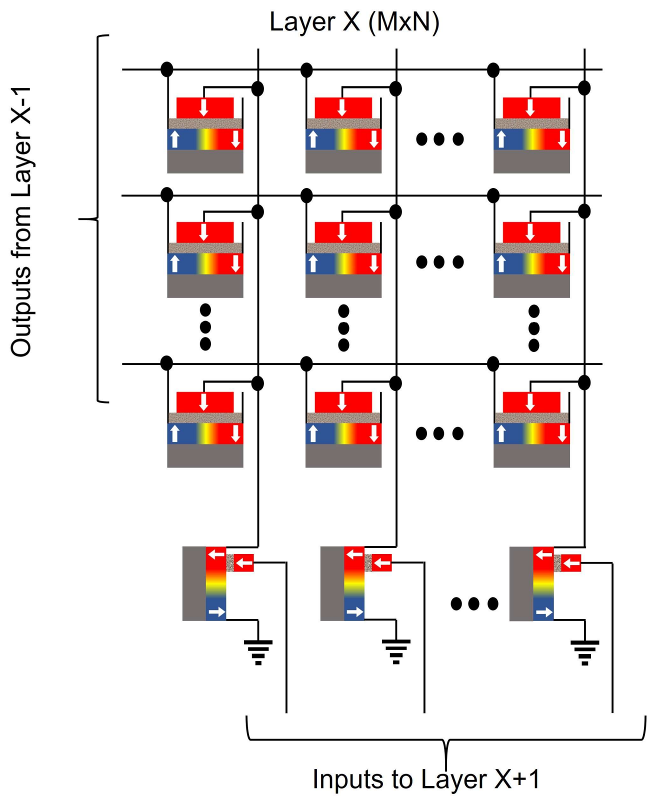

Fig. 5. Spintronic neural network layer using the DW-MTJ neuron of Fig. 2 and the DW-MTJ synapse of Fig. 1. The synapses at the intersections of word and bit lines provide weights between two individual neurons, and the neurons of one layer provide the inputs to another layer.

additional ferromagnet itself, and one being an electrically insulating layer between this ferromagnet and the neurons. The anisotropy gradient neuron, on the other hand, can be implemented through Ga^+ ion irradiation of the DW track. This has the advantage of minimizing the number of material layers, but it does require additional fabrication steps in order to irradiate the track. Finally, the shape gradient neuron also does not require any additional material layers, but it requires lithography for a non-rectangular shape, and will have a larger area overhead. Although it is currently unclear which of these approaches is most effective, further advances in material science and the fabrication of beyond-CMOS devices will shed light on this matter.

C. *Firing with a DW-MTJ Neuron*

When a sufficient amount of current has been integrated, the DWs in the artificial neurons reviewed in this work will have shifted underneath the MTJs. This will alter the resistance states of the devices, causing output spikes similar to those of standard LIF neurons.

IV. CMOS-Free Multilayer Spintronic Perceptron

The development of these spintronic neurons and synapses enables the construction of CMOS-free spintronic neural network layers, as shown in Figure 5. While spintronic neural networks have previously been considered [8], significant CMOS circuitry was required in addition to the spintronic synapses and neurons in order to implement leaking.

V. Conclusions

This work reviews three novel DW-MTJ neurons that, in conjunction with DW-MTJ-based synapses, enable a purely spintronic neural network. These LIF neurons intrinsically provide the leaking, integrating, and firing capabilities, thereby eschewing the need for additional CMOS circuitry. By exploiting biomimetic synapses and neurons in a simplified fabrication, these devices promise significant advances for efficient machine learning and artificial intelligence applications.

References

[1] Delorme, A., Gautrais, J., Rullen, R. V., Thorpe, S., “SpikeNET: A simulator for modeling large networks of integrate and fire neurons,” *Neurocomputing* vol. 26-27, pp. 989–996, 1999.

[2] Han, S., Mao, H., Dally, W. J., “Deep Compression: Compressing Deep Neural Networks with Pruning, Trained Quantization, and Huffman Coding,” *ICLR* 2016.

[3] Sengupta, B., Stemmler, M.B., “Power Consumption During Neuronal Computation,” *Proceedings of the IEEE*, vol. 102, no. 5, pp. 738-750, 2014

[4] Akopyan, F., Sawada, J., Cassidy, A., Alvarez-Icaza, R., Arthur, J., Merolla, P., Imam, N., Nakamura, Y., Datta, P., et al., “TrueNorth: Design and Tool Flow of a 65 mW 1 Million Neuron Programmable Neurosynaptic Chip,” *IEEE Transactions on Computer-Aided Design of Integrated Circuits and Systems,* vol. 34, no. 10, pp. 1537–1557, 2015.

[5] Merolla, P. A., Arthur, J. V., Alvarez-Icaza, R., Cassidy, A. S., Sawada, J., Akopyan, F., Jackson, B. L., Imam, N., Guo, C., et al., “A million spiking-neuron integrated circuit with a scalable communication network and interface,” *Science,* vol. 345, no. 6197, pp. 668–673, 2014.

[6] D. B. Strukov, G. S. Snider, D. R. Stewart, and R. S. Williams, “The missing memristor found,” *Nature*, vol. 453, pp. 80–83, 2008.

[7] Lin, Y.-P., Bennett, C. H., Cabaret, T., Vodenicarevic, D., Chabi, D., Querlioz, D., Jousselme, B., Derycke, V., Klein, J.-O., “Physical Realization of a Supervised Learning System Built with Organic Memristive Synapses,” *Scientific Reports,* vol. 6, no. 1, 2016.

[8] A. Sengupta, Y. Shim, and K. Roy, “Proposal for an all-spin artificial neural network: Emulating neural and synaptic functionalities through domain wall motion in ferromagnets,” *IEEE Trans. Biomed. Circuits Syst.*, vol. 10, no. 6, pp. 1152–1160, 2016.

[9] Sharad, M., Fan, D., Aitken, K., Roy, K., “Energy-Efficient Non-Boolean Computing With Spin Neurons and Resistive Memory,” *IEEE Transactions on Nanotechnology,* vol. 13, no. 1, pp. 23–34, 2014.

[10] S. Dutta, S. A. Siddiqui, F. Buttner, L. Liu, C. A. Ross, and M. A. Baldo, “A logic-in-memory design with 3-terminal magnetic tunnel junction function evaluators for convolutional neural networks,” *NANOARCH*, 2017.

[11] X. Chen, W. Kang, D. Zhu, X. Zhang, N. Lei, Y. Zhang, Y. Zhou, and W. Zhao, “A compact skyrmionic leaky–integrate–fire spiking neuron device,” *Nanoscale*, vol. 10, no. 13, pp. 6139–6146, 2018.

[12] N. Hassan, X. Hu, L. Jiang-Wei, W. H. Brigner, O. G. Akinola, F. Garcia-Sanchez, M. Pasquale, C. H. Bennett, J. A. C. Incorvia, J. S. Friedman, “Magnetic domain wall neuron with lateral inhibition,” *J. Appl. Phys.*, vol. 124, no. 15, p. 152127, 2018.

[13] W. H. Brigner, X. Hu, N. Hassan, C. H. Bennett, J. A. C. Incorvia, F. Garcia-Sanchez, and J. S. Friedman, “Graded-Anisotropy-

Induced Magnetic Domain Wall Drift for an Artificial Spintronic Leaky Integrate-and-Fire Neuron," *IEEE Journal on Exploratory Solid-State Computational Devices and Circuits*, vol. 5, no. 1, pp. 19–24, 2019.

[14] W. H. Brigner, N. Hassan, L. Jiang-Wei, X. Hu, D. Saha, C. H. Bennett, M. J. Marinella, J. A. C. Incorvia, F. Garcia-Sanchez, and J. S. Friedman, "Shape-Based Magnetic Domain Wall Drift for an Artificial Spintronic Leaky Integrate-and-Fire Neuron," *IEEE Transactions on Electron Devices*, vol. 66, no. 11, pp. 4970-4975, 2019.

[15] Y. Sun, C. R. Sullivan, W. Li, D. Kopp, F. Johnson, S. T. Taylor, "Soft magnetic properties of obliquely deposited Co–Zr–O films", *IEEE Trans. Magn*., vol. 43, no. 12, pp. 4060-4063, 2007.

[16] N. N. Phuoc, L. T. Hung, C. K. Ong, "FeCoHfN thin films fabricated by co-sputtering with high resonance frequency", *J. Alloys Compounds*, vol. 509, no. 9, pp. 4010-4013, 2011.

[17] S. Li, Z. Huang, J.-G. Duh, M. Yamaguchi, "Ultrahigh-frequency ferromagnetic properties of FeCoHf films deposited by gradient sputtering", *Appl. Phys. Lett.*, vol. 92, no. 9, 2008.